Systematic higher order nonlinear analysis of power systems operating under perturbation conditions

Journal Article

Author(s):
Rodriguez-Villalón, Osvaldo; Medina, Aurelio

Publication date:
2017-03

Permanent link:
https://doi.org/10.3929/ethz-b-000119652

Originally published in:
Electrical Engineering 99(1), https://doi.org/10.1007/s00202-016-0400-7

Electr Eng (2017) 99:141–159
DOI 10.1007/s00202-016-0400-7

ORIGINAL PAPER

Systematic higher order nonlinear analysis of power systems operating under perturbation conditions

O. Rodriguez-Villalon[1,2] · **A. Medina**[3]

Received: 2 September 2015 / Accepted: 3 August 2016 / Published online: 19 August 2016

Abstract In this paper, the modal series method is revisited and an extension on the method to include higher order terms is proposed. This proposal is based on the introduction of the multidimensional Laplace transform and association of variables theorems to deduce the analytical closed-form solution when it is applied to the analysis of a nonlinear power system model. The method is systematic and can incorporate higher order terms to the modal analysis to determine nonlinear modal interaction. When the power system is operating under stressed conditions, such as an increase in load demand, it results very important to consider the oscillations due to its nonlinear nature. Thus, the method is carefully exemplified with the application to the synchronous machine-infinite busbar power system operating under stress conditions. The oscillations produced during changes in its operation are analyzed as well as the nonlinear interaction through nonlinear indices and nonlinear participation factors. The time domain responses are compared between linear approximation, modal series, normal forms method and the direct numerical full solution of the nonlinear power system model.

Keywords Modal series methods · Nonlinear dynamic systems · Multidimensional Laplace transforms

✉ O. Rodriguez-Villalon
osvaldo@ugto.mx

1 División de Ingenierías del Campus Irapuato-Salamanca (DICIS), Departamento de Ingeniería Eléctrica, Universidad de Guanajuato, 36885 Salamanca, Guanajuato, Mexico

2 Power Systems Laboratory, ETH Zurich, Zurich, Switzerland

3 División de Estudios de Posgrado, Facultad de Ingeniería Eléctrica, Universidad Michoacana de San Nicolás de Hidalgo (UMSNH), 58000 Morelia, Michoacán, Mexico

1 Introduction

The nonlinear phenomena associated to the operation of power systems have been deeply analyzed [1–4]. In our days, the nonlinear system behavior is an increasingly important area of research, with applications in many areas of power system analysis and control. Efforts on developing methods which allow to incorporate the nonlinear effects of dynamic systems have been developed [1–5].

Over the last decades, the method based on normal forms (NF) of vector fields has been strongly used as an analytical tool to study the nonlinear effects in power systems. Some contributions over this platform have been focused on predicting interarea separations [1], power system control design [2], interarea modes phenomenon [3,4], incorporation of FACTS devices [5]. In [6], authors proposed the study of power systems through computation of real NF under resonant conditions; here the analytical procedure followed is derived from normal form nonlinear transformation which converts the system into minimal normal form, but in addition, the converted system is not transformed into a diagonal form. In [7], stability indexes of power system oscillation taking into consideration nonlinearity using NF is proposed. They obtain a solution under non-resonance and resonance modal cases and proposed indices to evaluate the effects on nonlinear system's interaction. In [8], a control application is proposed based on NF method, extending the formulation to reduce the nonlinear characteristics of the power system and analyzing the excitation system perturbations.

On the other side, the method of modal series (MS) has been introduced as an alternative method to incorporate nonlinear effects in stressed power systems [9,10]. The contribution [10] recalls the research reported in [9], with some additions of modal series applications to the power systems previous considered. The characteristics of the method allows the power systems analysis even in the presence of modal resonance conditions. However, an extension to include higher order terms has not been considered so far.

Other recent developments based on modal series have been focused on comparing responses and characteristics with respect to normal forms method [11] and on identifying nonlinear characteristics due to torsional interactions nonlinear indices [12]. The modal expansion procedure is in addition extended to the case of multidimensional nonlinear systems described by forced nonlinear differential equations [13], and also incorporating UPFC controller to take into account the damping characteristics due to nonlinear contributions to the power system [14].

In this paper, the modal series method and its fundamental theory is revisited. First, a review of existing modal analysis techniques is presented with emphasis on the derivation of closed-form analytical expressions with explicit dependence on modal parameters, system structure, and initial conditions. Then, a general procedure based on the multidimensional Laplace transform is proposed to analyze complex system representations and to obtain a general form to incorporate higher order terms in the modal series. The application of multidimensional Laplace transform and its interrelationship with Volterra series allow the incorporation of a systematic procedure to determine higher order terms in the modal series. Also, the method of association of variables and its theorems are of great advantage to determine such terms. These theorems are well documented in [15–18]. Introduction of nonlinear interaction indices and nonlinear participation factors are incorporated to characterize the nonlinear modal interaction of the power system. Time domain responses are compared against linear approximation, normal forms solution and the full numerical solution of the dynamic model represented by a set of ordinary differential equations.

The rest of the paper content is structured as follows: Section 2 gives the core of the modal series method through the linearization process based on Taylor series expansion and Jordan canonical form transformation; Section 3 establishes the basis to obtain higher order terms by incorporating the multidimensional Laplace transform and association of variables; in Sect. 4, the method of higher order modal series is applied to the SMIB test system describing in an analytical way each step followed by the modal series method. In Sect. 5, the numerical results of the power system tests showing a comparative analysis with respect to the full numerical solution and the oscillations observed by the modal series method solution are detailed. Nonlinear analysis interaction is carried out in Sect. 6, followed by a brief discussion about advantages and disadvantages of the method in Sect. 7, finishing with the conclusions in Sect. 8.

2 The modal series background

A nonlinear dynamical system can be defined by a set of n-dimensional ordinary differential equations, which can be either homogeneous or no homogeneous, depending on the input variables response, i.e.,

$$\dot{\mathbf{x}} = \mathbf{f}(\mathbf{x}, \mathbf{u}) \tag{1}$$

In (1), $\mathbf{x}$ is defined as an n-dimensional vector of dynamic system states, defined over the field $\mathbf{f} : R^n \rightarrow R^n$. In addition, (1) can incorporate the input variables of the dynamic system $\mathbf{u} \in \Re^m$, which is the control vector input.

The dynamic system (1) can be expanded around an initial equilibrium point X_{SEP} (this constraint warranties the existence of solution to the nonlinear system) following the Taylor series definition, that is,

$$\begin{aligned}\dot{x}_i &= A_i x + \frac{1}{2}\sum_{k=1}^{n}\sum_{l=1}^{n} F_{2kl}^{i} x_k x_l \\ &\quad + \frac{1}{6}\sum_{p=1}^{n}\sum_{q=1}^{n}\sum_{r=1}^{n} F_{3pqr}^{i} x_p x_q x_r + \cdots \end{aligned} \tag{2}$$

Some important definitions are obtained from this expansion:

- A_i is defined as the ith row of the Jacobian matrix (state matrix) or $A_i = (\partial f_i/\partial x)|_{X_{\text{SEP}}}$ of $f(x)$. This term corresponds to the linear component of the original nonlinear dynamic system.
- F coefficients are related to the nonlinear components of the nonlinear dynamic system (1).
- F_{2kl}^{i} is the klth second order term associated with the ith state or $F_{2kl}^{i} = (\partial^2 f_i/\partial x_k \partial x_l)|_{X_{\text{SEP}}}$ (*Hessian* of $f(x)$).
- Following the same reasoning, F_{3pqr}^{i} is the pqrth third order term associated with the ith state or $F_{3pqr}^{i} = (\partial^3 f_i/\partial x_p \partial x_q \partial x_r)|_{X_{\text{SEP}}}$.

No inputs are considered in this research. However, it is possible to incorporate input functions effects on the modal series method [19].

The state matrix or Jacobian matrix $\mathbf{A}$ has an eigenvalue set $\{\lambda_1 \quad \lambda_2 \quad \cdots \quad \lambda_n\}$ with right eigenvectors $\mathbf{U}$ and reciprocal left eigenvectors $\mathbf{V} = \mathbf{U}^{-1}$ [3]. The procedure followed before the introduction of modal series analysis indicates that a linear change of coordinates can be performed. Basically, this change corresponds to the so called Jordan canonical form, which is a kind of linear transformation of the expanded dynamic system (2), characterized by the application of the new definition $\mathbf{x} = \mathbf{U}\mathbf{y}$. Now the system is converted in the "new states" given by,

$$\dot{y}_j = \lambda_j y_j + \sum_{k=1}^{n}\sum_{l=1}^{n} C_{kl}^{j} y_k y_l + \sum_{p=1}^{n}\sum_{q=1}^{n}\sum_{r=1}^{n} D_{pqr}^{j} y_p y_q y_r + \cdots \quad j = 1, \ldots, n \tag{3}$$

where,

$$C_{kl}^{j} = \frac{1}{2}\sum_{p=1}^{n} V_{jp}^{T}[U^{\mathrm{T}} H^{P} U]$$

coefficients of second order terms

$$D_{pqr}^{j} = \frac{1}{6}\sum_{P=1}^{N}\sum_{Q=1}^{N}\sum_{R=1}^{N} P_{PQR}^{j} V_p^P V_q^Q V_r^R$$

coefficients of third order terms.

Please observe that terms above third order are assumed to be negligible, also input variables can be considered rather leaving their effects to other contributions further explored by the authors. Additionally, a forced response of the nonlinear system can be also incorporated, thus allowing to represent transfer functions [19].

Under this truncation, it is possible to approximate the system behavior; low-dimensional representations can be used. Similar developments in this field have been focused on normal form analysis [20]. The system developed through (3) represents the core of the modal series method which is detailed in the next section.

3 Higher order modal series deduction

In this section, the modal series method is revisited, and the multidimensional Laplace domain comprised to deduce higher components of the modal series.

Considering the nonlinear system described by the nonlinear model (3) and from Volterra series theory, we assume that the system response $y_j(t)$ can be expressed as an infinite series [16], i.e.,

$$y_j(t) = \sum_{k=1}^{\infty} \varepsilon^k y_j^k(t) \tag{4}$$

Substituting (4) and its derivative into (3), considering the case without input functions effects ($u_m = 0$), and equating the coefficients of equal powers of ε, yields the following set of linear equations

$$\begin{aligned}
\dot{y}_j(t) &= \lambda_j y_j(t)\\
\dot{y}_j^2(t) &= \lambda_j y_j^2(t) + \sum_{k=1}^{n}\sum_{l=1}^{n} C_{kl}^{j} y_k(t)\, y_l(t)\\
\dot{y}_j^3(t) &= \lambda_j y_j^3(t) + \sum_{k=1}^{n}\sum_{l=1}^{n} C_{kl}^{j}[y_k^2(t) y_l(t) + y_k(t) y_l^2(t)]\\
&\quad + \sum_{p=1}^{n}\sum_{q=1}^{n}\sum_{r=1}^{n} D_{pqr}^{j} y_p^1(t) y_q^1(t)\, y_r^1(t)\\
&\vdots
\end{aligned} \tag{5}$$

These equations can be conveniently analyzed using the proposed framework. Straightforward application of the Laplace transform means a systematic procedure, which allows the analytical solution of the nonlinear system assuming uncoupled each term (linear and nonlinear terms) yields,

$$\begin{aligned}
& s_1 Y_j^1(s) - Y_j^1(0) = \lambda_j Y_j^1(s)\\
& (s_1+s_2)\, Y_j^2(s_1,s_2) = \lambda_j Y_j^2(s_1,s_2)\\
& \quad + \sum_{k=1}^{n}\sum_{l=1}^{n} C_{kl}^{j} Y_k^1(s_1)\, Y_l^1(s_2)\\
& (s_1+s_2+s_3)\, Y_j^3(s_1,s_2,s_3) = \lambda_j Y_j^3(s_1,s_2,s_3)\\
& \quad + \sum_{k=1}^{n}\sum_{l=1}^{n} C_{kl}^{j}\Big[Y_k^2(s_1,s_2)\, Y_l^1(s_3)\\
& \quad + Y_k^1(s_1)\, Y_l^2(s_2,s_3)\Big]\\
& \quad \times \sum_{p=1}^{n}\sum_{q=1}^{n}\sum_{r=1}^{n} D_{pqr}^{j}\Big[Y_p^1(s_1)\, Y_q^1(s_2)\, Y_r^1(s_3)\Big]\\
& \quad \vdots
\end{aligned} \tag{6}$$

The system obtained in (6) may be efficiently solved by applying an approach based on multidimensional Laplace transform analysis.

3.1 Multidimensional Laplace transform

Let $f(t_1, t_2, \ldots, t_n)$ be a real or complex-valued function of n independent real variables, $t_1, t_2, \ldots, t_n$ The Laplace transform, $F(s_1, s_2, \ldots, s_n)$ of $f(t_1, t_2, \ldots, t_n)$, is defined by the integral [16] as,

$$F(s_1, s_2, \ldots, s_n) = \int_0^{\infty} \cdots \int_0^{\infty} \mathrm{e}^{\left(-\sum_{j=1}^{n} s_j t_j\right)} \times f(t_1, t_2, \ldots, t_n)\, \mathrm{d}t_1\, \mathrm{d}t_2 \cdots \mathrm{d}t_n \tag{7}$$

where the transform is a function of n variables.

Following the same reasoning as the single variable Laplace transform, an inverse Laplace can be obtained as it appears indicated in the flow chart of Fig. 1. The scheme shows the application of the multidimensional Laplace and association of variables theorem.

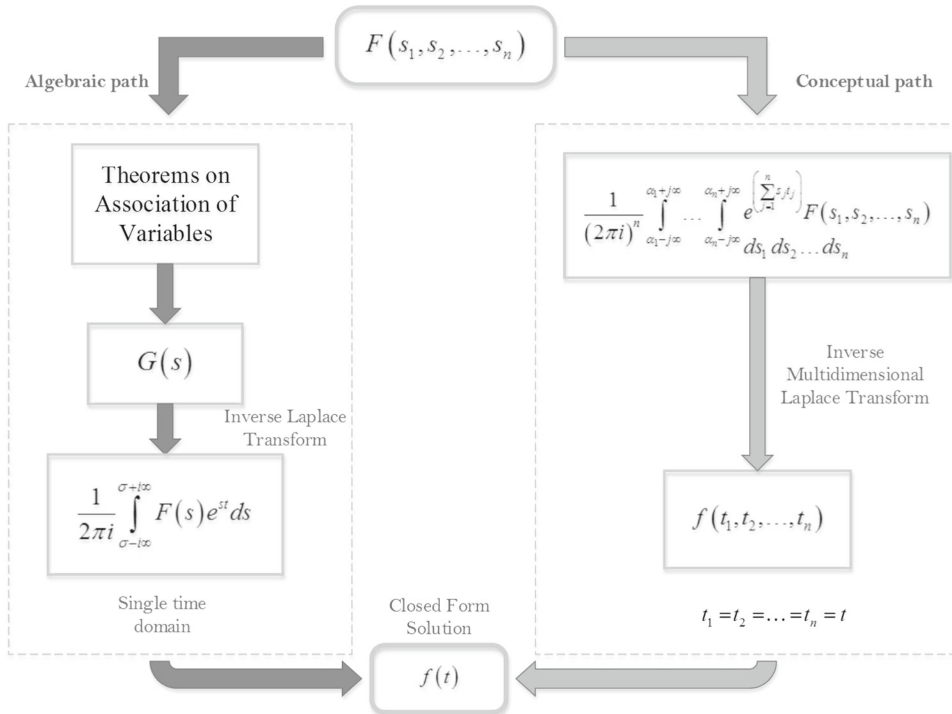

Fig. 1 Multidimensional Laplace transform flow chart

According to the flow chart, the process of solution can be followed in two different alternatives, i.e., from the multidimensional Laplace kernels, the association of variables can be applied thus resulting in a single Laplace expression, that is solved using inverse Laplace transform; a different alternative indicates that it is possible to determine a multidimensional time function using the inverse of the multidimensional Laplace transform. The inverse of the n-dimensional Laplace transform for a single variable is,

$$g(t) = f(t_1, t_2, \ldots, t_n)\big|_{t=t_1=t_2=\cdots=t_n=t} \tag{8}$$

Equation (8) indicates that a multi-time nonlinear system can be simplified into a single time domain variable. Thus, a transformed function in n-dimensions is first evaluated for a single transformed variable and then a single dimensional inverse Laplace transform is applied. The procedure to find $Y(s)$ from $F(s_1, s_2, \ldots, s_n)$ is known as the *method of association of variables* [15], as it was indicated above.

One of the main advantages of the multidimensional Laplace concept is that it incorporates the cross-frequency-relationship in the nonlinear system from an analytical expression. Multidimensional Laplace kernels are expressed in terms on multi-Laplace variables, which represents the different frequency characteristics that are inherent in nature of the dynamic system. A result in these terms means a combination between variables, which is traduced into a combination between frequency characteristics of each order. This characteristic is therefore yielded to the modal series solution, in which the time domain solution, as it will be demonstrated further, is a combination of several frequency contributions included in the modal combination.

On the other side, some theorems have been developed to solve different kind of nonlinear equation sets. It is possible to determine the better option to deal with the necessary multidimensional Laplace expression to be solved. In [17], these aspects are defined in detail.

3.2 Second and higher order approximations

From (6), it is possible to determine the first, second and higher order terms. Here, the systematic procedure may be defined following the flow chart of Fig. 2.

The process starts with the linear transformation based on the right eigenvectors, thus converting the system in the new set of variables y^j. Please observe that linear terms are uncoupled, and the higher order terms are coupled and in their own are function of the previous order (second order terms are function of first order, third order are function of first and second order and so on).

Also important in this systematic procedure is the application of multidimensional Laplace transform to the coupled higher order terms, which are solved afterwards by the application of inverse Laplace domain and association of variables to determine a time domain solution. Details of this deduction are extended in Appendix A.

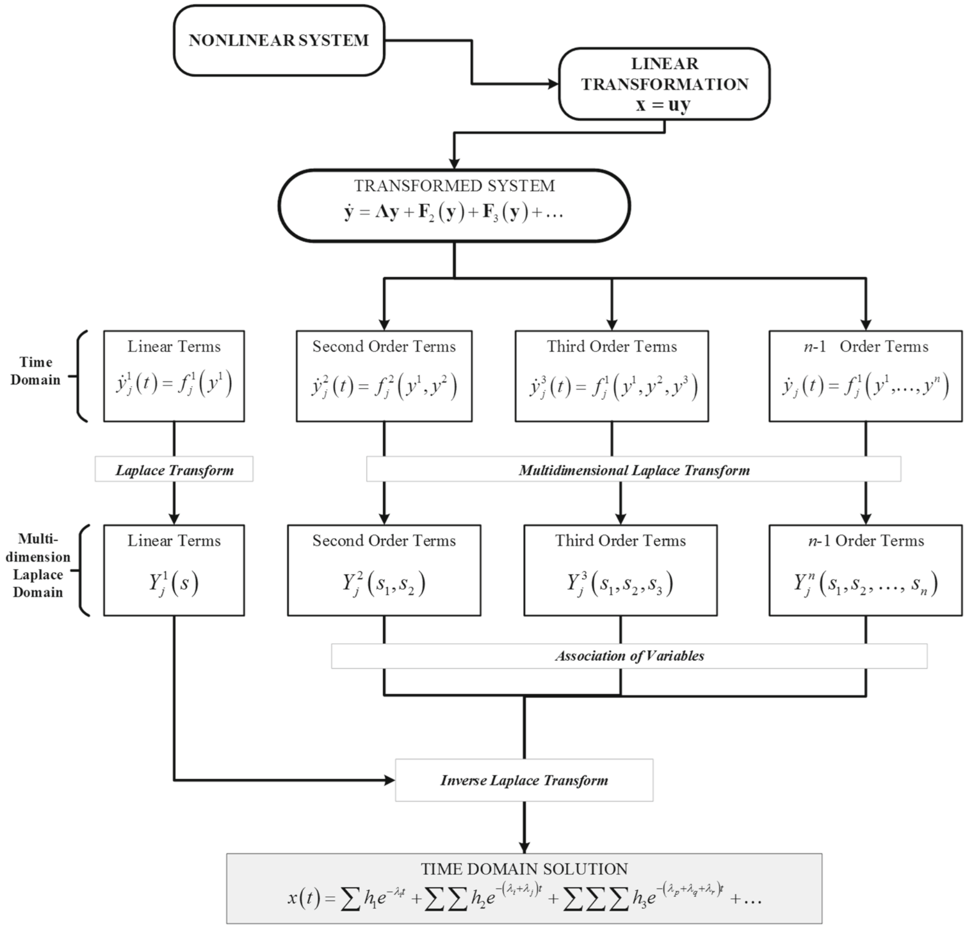

Fig. 2 Flow chart of the modal series method deduction

Performing the inversion with respect to s, the closed-form solutions are obtained as,

$$y_j^2(t) = \sum_{k=1}^{n}\sum_{l=1}^{n} C_{kl}^{j} y_k(0)\, y_l(0) \frac{1}{(\lambda_k + \lambda_l - \lambda_j)} \times \left[e^{(\lambda_k+\lambda_l)t} - e^{\lambda_j t} \right] \tag{9}$$

$$\begin{aligned} y_j^3(t) = &\sum_{k=1}^{n}\sum_{l=1}^{n}\sum_{p=1}^{n}\sum_{q=1}^{n} C_{kl}^{j} C_{pq}^{k} Y_p^1(0)\, Y_q^1(0)\, Y_l^1(0) \\ &\times \left\{ \frac{1}{(\lambda_j - \lambda_p - \lambda_q - \lambda_l)} \left[\frac{1}{(\lambda_j - \lambda_l - \lambda_k)} e^{\lambda_j t} \right.\right. \\ &\left.\left. - \frac{1}{(\lambda_p + \lambda_q - \lambda_k)} e^{(\lambda_p+\lambda_q+\lambda_l)t} \right]\right\} \\ &+ \sum_{k=1}^{n}\sum_{l=1}^{n}\sum_{p=1}^{n}\sum_{q=1}^{n} C_{kl}^{j} C_{pq}^{l} Y_k^1(0)\, Y_p^1(0)\, Y_q^1(0) \\ &\times \left\{ \frac{1}{(\lambda_j - \lambda_p - \lambda_q - \lambda_k)} \frac{1}{(\lambda_p + \lambda_q - \lambda_l)} \right. \\ &\left. \times \left[e^{\lambda_j t} - e^{(\lambda_p+\lambda_q+\lambda_k)t} \right] \right\} \\ &+ \sum_{p=1}^{n}\sum_{q=1}^{n}\sum_{r=1}^{n} D_{pqr}^{j} Y_p^1(0)\, Y_q^1(0)\, Y_r^1(0) \\ &\times \frac{1}{(\lambda_j - \lambda_p - \lambda_q - \lambda_r)} \left[e^{(\lambda_j)t} - e^{(\lambda_p+\lambda_q+\lambda_r)t} \right] \end{aligned} \tag{10}$$

which after some manipulations yields,

$$\begin{aligned} y_j(t) = &\left(y_j(0) - \sum_{k=1}^{n}\sum_{l=1}^{n} h_{2kl}^{j} y_k(0)\, y_l(0) \right) e^{\lambda_j t} \\ &+ \sum_{k=1}^{n}\sum_{l=1}^{n} h_{2kl}^{j} y_k(0)\, y_l(0) e^{(\lambda_k+\lambda_l)t} \\ &+ \sum_{p=1}^{n}\sum_{q=1}^{n}\sum_{r=1}^{n} h_{3pqr}^{j} y_p^1(0)\, y_q^1(0)\, y_r^1(0) \\ &\times \left[e^{(\lambda_j)t} - e^{(\lambda_p+\lambda_q+\lambda_r)t} \right] \\ &+ \sum_{k=1}^{n}\sum_{l=1}^{n}\sum_{p=1}^{n}\sum_{q=1}^{n} \frac{y_p^1(0)\, y_q^1(0)\, y_l^1(0)}{(\lambda_j - \lambda_p - \lambda_q - \lambda_l)} \\ &\times \left[h_{2kl}^{j} e^{\lambda_j t} - h_{2pq}^{l} e^{(\lambda_p+\lambda_q+\lambda_l)t} \right] \end{aligned}$$

$$+\sum_{k=1}^{n}\sum_{l=1}^{n}\sum_{p=1}^{n}\sum_{q=1}^{n} h_{2pq}^{l} C_{kl}^{j} \frac{y_k^1(0)\, y_p^1(0)\, y_q^1(0)}{\left(\lambda_j-\lambda_p-\lambda_q-\lambda_k\right)} \times\left[\mathrm{e}^{\lambda_j t}-\mathrm{e}^{\left(\lambda_p+\lambda_q+\lambda_k\right) t}\right] \tag{11}$$

and

$$\begin{aligned} x_i(t) &= \sum_{j=1}^{n}\left(u_{ij} y_j(0)-\sum_{k=1}^{n}\sum_{l=1}^{n} u_{ij} h_{2kl}^{j} y_k(0)\, y_l(0)\right)\mathrm{e}^{\lambda_j t} \\ &+\sum_{j=1}^{n}\sum_{k=1}^{n}\sum_{l=1}^{n} u_{ij} h_{2kl}^{j} y_k(0)\, y_l(0)\, \mathrm{e}^{(\lambda_k+\lambda_l)t} \\ &+\sum_{p=1}^{n}\sum_{q=1}^{n}\sum_{r=1}^{n} u_{ij} h_{3pqr}^{j} y_p^1(0)\, y_q^1(0)\, y_r^1(0) \\ &\times\left[\mathrm{e}^{(\lambda_j)t}-\mathrm{e}^{(\lambda_p+\lambda_q+\lambda_r)t}\right] \\ &+\sum_{k=1}^{n}\sum_{l=1}^{n}\sum_{p=1}^{n}\sum_{q=1}^{n} u_{ij}\frac{y_p^1(0)\, y_q^1(0)\, y_l^1(0)}{\left(\lambda_j-\lambda_p-\lambda_q-\lambda_l\right)} \\ &\times\left[h_{2kl}^{j}\mathrm{e}^{\lambda_j t}-h_{2pq}^{l}\mathrm{e}^{(\lambda_p+\lambda_q+\lambda_l)t}\right] \\ &+\sum_{k=1}^{n}\sum_{l=1}^{n}\sum_{p=1}^{n}\sum_{q=1}^{n} u_{ij} h_{2pq}^{l} C_{kl}^{j}\frac{y_k^1(0)\, y_p^1(0)\, y_q^1(0)}{\left(\lambda_j-\lambda_p-\lambda_q-\lambda_k\right)} \\ &\times\left[\mathrm{e}^{\lambda_j t}-\mathrm{e}^{(\lambda_p+\lambda_q+\lambda_k)t}\right] \end{aligned} \tag{12}$$

In the above equations, the second and third order nonlinear coefficients are defined by

$$h_{2kl}^{j}=\frac{C_{kl}^{j}}{\lambda_k+\lambda_l-\lambda_j} \tag{13}$$

$$h_{3pqr}^{j}=\frac{D_{pqr}^{j}}{\left(\lambda_j-\lambda_p-\lambda_q-\lambda_r\right)} \tag{14}$$

The procedure can be indefinitely continued to determine higher order nonlinear expressions in terms of the lower-order modal expansions. The coefficients represent the modal interaction between modes and physical characteristics of the nonlinear system since they are defined from the individual parameters of the dynamic system and also by modal characteristics.

In Sect. 6, these coefficients are taken into account when the nonlinear participation factors are analyzed.

3.3 Modal series closed-form solution under resonance condition

Recalling the nonlinear coefficients h_2 defined by (13), the resonance condition is established as,

$$\lambda_k+\lambda_l-\lambda_j=0 \tag{15}$$

Thus, the Laplace transform kernels considering the resonance assumption are obtained. According to the resonance condition constraint, the kernel is defined as,

$$Y_j^2(s_1,s_2)=\sum_{k=1}^{n}\sum_{l=1}^{n} C_{kl}^{j} Y_k^1(0)\, Y_l^1(0) \times\frac{1}{(s_1+s_2-\lambda_k-\lambda_l)(s_1-\lambda_k)(s_2-\lambda_l)} \tag{16}$$

which is associated in terms of Laplace domain as,

$$Y_j^1(s)=\frac{Y_j^1(0)}{(s_1-\lambda_k-\lambda_l)}$$

Obtaining a time domain solution through inverse Laplace leads to,

$$y_j^1(t)=y_j^1(0)\,\mathrm{e}^{\lambda_j t} \tag{17}$$

The second order kernel, is associated following the rule of association of variables detailed in Appendix A as,

$$H_2(s)=\frac{1}{\left(s-\lambda_j\right)^2} \tag{18}$$

from which the time domain solution solving the inverse Laplace is,

$$h_2(t)=t\mathrm{e}^{\lambda_j t}$$

Thus, the complete closed-form solution when a modal resonance condition is presented takes the form,

$$\begin{aligned} x_j(t) &= u_{ij} y_j(0)\,\mathrm{e}^{\lambda_j t}+\sum_{k=1}^{n}\sum_{l=1}^{n} C_{kl}^{j} y_k(0)\, y_l(0)\, t\mathrm{e}^{\lambda_j t} \\ &+\sum_{k=1}^{n}\sum_{l=1}^{n} u_{ij} h_{2kl}^{j} y_k(0)\, y_l(0)\, t^2\mathrm{e}^{(\lambda_k+\lambda_l)t} \\ &+\sum_{p=1}^{n}\sum_{q=1}^{n}\sum_{r=1}^{n} u_{ij} h_{3pqr}^{j} y_p^1(0)\, y_q^1(0)\, y_r^1(0) \\ &\times\left[t\mathrm{e}^{(\lambda_j)t}-t^3\mathrm{e}^{(\lambda_p+\lambda_q+\lambda_r)t}\right] \\ &+\sum_{k=1}^{n}\sum_{l=1}^{n}\sum_{p=1}^{n}\sum_{q=1}^{n} u_{ij}\frac{y_p^1(0)\, y_q^1(0)\, y_l^1(0)}{\left(\lambda_j-\lambda_p-\lambda_q-\lambda_l\right)} \\ &\times\left[h_{2kl}^{j} t\mathrm{e}^{\lambda_j t}-t^3 h_{2pq}^{l}\mathrm{e}^{(\lambda_p+\lambda_q+\lambda_l)t}\right] \\ &+\sum_{k=1}^{n}\sum_{l=1}^{n}\sum_{p=1}^{n}\sum_{q=1}^{n} u_{ij} h_{2pq}^{l} C_{kl}^{j}\frac{y_k^1(0)\, y_p^1(0)\, y_q^1(0)}{\left(\lambda_j-\lambda_p-\lambda_q-\lambda_k\right)} \\ &\times\left[t\mathrm{e}^{\lambda_j t}-t^3\mathrm{e}^{(\lambda_p+\lambda_q+\lambda_k)t}\right] \end{aligned} \tag{19}$$

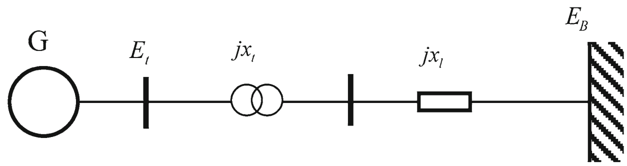

Fig. 3 Synchronous machine-infinite busbar power system

4 Power system modeling by higher order modal series

The application of the modal series method including higher order terms is demonstrated with the synchronous machine-infinite busbar test power system illustrated in Fig. 3.

A third order generator model is assumed, which incorporates the dynamic of the electromechanical system. The differential equations are [21],

$$\begin{aligned} \frac{dE_q'}{dt} &= -\left(\frac{1}{T_{d0}'}\right)\left[E_q' + \left(x_d - x_d'\right) I_d - E_{fd}\right] = f_1 \\ \frac{d\delta}{dt} &= \omega - \omega_0 = f_2 \\ \frac{d\omega}{dt} &= \left(\frac{\omega_0}{2H}\right)[T_M - \{E_q' I_q + (x_q - x_d')I_d I_q \\ &\quad - D(\omega - \omega_0)\}] = f_3 \end{aligned} \tag{20}$$

where δ represents the rotor angular position in electric radians with reference to the infinite busbar, ω is the rotor speed in rad/s, P_m is the input mechanical power in p.u., D_m is the damping coefficient in torque p.u./speed p.u. and H is the inertia constant in MWs/MVA. Data used in the experiment are detailed in Appendix C.

Eliminating the stator resistances effects, the algebraic equations are,

$$-(x_q + x_t + x_l)I_q + V_b \sin\delta = 0 \tag{21}$$

$$(x_d' + x_t + x_l)I_d - E_q' + V_b \cos\delta = 0 \tag{22}$$

The linearization of the system around a stable equilibrium point has the form,

$$\dot{\mathbf{x}} = f_1(\mathbf{x}) + f_2(\mathbf{x}) + f_3(\mathbf{x}) + \cdots \tag{23}$$

with $\mathbf{x} = [x_1 \quad x_2 \quad x_3]^{\mathrm{T}} = [E_q' \quad \delta \quad \omega]^{\mathrm{T}}$.

This dynamic system has the equilibrium point,

$$\begin{aligned} x_0 &= [E_{q0}' \quad \delta_0 \quad \omega_0]^{\mathrm{T}} \\ x_0 &= \begin{bmatrix} V_b \cos(\delta_0 - \theta_{vs}) + (x_t + x_l + x_d')I_d \\ \mathrm{angle}(V_b e^{j\theta_{vs}} + j(x_q + x_t + x_l)I_G e^{j\gamma}) \\ \omega_0 \end{bmatrix} \end{aligned} \tag{24}$$

The linear and nonlinear functions defined by (23) for which it is necessary to determine their closed-form solutions are obtained next. Information of first, second and third order terms is given in Appendix B

4.1 Modal series solution

Based on (3) which links the relationship between the transformed variables with Jordan canonical form, the system (23) is transformed, resulting in,

$$\dot{\mathbf{y}} = \mathbf{\Lambda y} + \mathbf{f_2}(\mathbf{y}) + \mathbf{f}_3(\mathbf{y}) \tag{25}$$

where,

$$\begin{aligned} \mathbf{f}_2(\mathbf{y}) &= \frac{1}{2}\mathbf{U}^{-1}\begin{bmatrix} (\mathbf{Uy})^{\mathbf{T}}\mathbf{H}_2^1\mathbf{Uy} \\ (\mathbf{Uy})^{\mathbf{T}}\mathbf{H}_2^2\mathbf{Uy} \\ (\mathbf{Uy})^{\mathbf{T}}\mathbf{H}_2^3\mathbf{Uy} \end{bmatrix} \\ &= \frac{1}{2}\begin{bmatrix} \sum_{k=1}^{N}\sum_{l=1}^{N} C_{kl}^1 y_k y_l \\ \sum_{k=1}^{N}\sum_{l=1}^{N} C_{kl}^2 y_k y_l \\ \sum_{k=1}^{N}\sum_{l=1}^{N} C_{kl}^3 y_k y_l \end{bmatrix} \end{aligned} \tag{26}$$

and

$$\begin{aligned} \mathbf{f}_3(\mathbf{x}) &= \frac{1}{6}\mathbf{U}^{-1}\begin{bmatrix} (\mathbf{Uy})^{\mathrm{T}}\mathbf{H}_3^1\begin{bmatrix} \mathbf{Uy} & \mathbf{0} & \mathbf{0} \\ \mathbf{0} & \mathbf{Uy} & \mathbf{0} \\ \mathbf{0} & \mathbf{0} & \mathbf{Uy} \end{bmatrix}\mathbf{Uy} \\ (\mathbf{Uy})^{\mathrm{T}}\mathbf{H}_3^2\begin{bmatrix} \mathbf{Uy} & \mathbf{0} & \mathbf{0} \\ \mathbf{0} & \mathbf{Uy} & \mathbf{0} \\ \mathbf{0} & \mathbf{0} & \mathbf{Uy} \end{bmatrix}\mathbf{Uy} \\ (\mathbf{Uy})^{\mathrm{T}}\mathbf{H}_3^3\begin{bmatrix} \mathbf{Uy} & \mathbf{0} & \mathbf{0} \\ \mathbf{0} & \mathbf{Uy} & \mathbf{0} \\ \mathbf{0} & \mathbf{0} & \mathbf{Uy} \end{bmatrix}\mathbf{Uy} \end{bmatrix} \\ \mathbf{f}_3(\mathbf{y}) &= \frac{1}{6}\begin{bmatrix} \sum_{k=1}^{n}\sum_{l=1}^{n}\sum_{m=1}^{n} D_{3klm}^1 y_k y_l y_m \\ \sum_{k=1}^{n}\sum_{l=1}^{n}\sum_{m=1}^{n} D_{3klm}^2 y_k y_l y_m \\ \sum_{k=1}^{n}\sum_{l=1}^{n}\sum_{m=1}^{n} D_{3klm}^3 y_k y_l y_m \end{bmatrix} \end{aligned} \tag{27}$$

where C_{kl}^j and D_{3klm}^j are defined in (4).

Once the nonlinear dynamic system has been transformed to the Jordan canonical form, the Laplace transformation has to be carried out. The system expressed in the Laplace domain represents the contributions of linear and nonlinear higher order terms, which have to be solved by association of variables theorems as described above. The full solution obtained for the nonlinear system is given by,

$$\begin{bmatrix} y_1(t) \\ y_2(t) \\ y_3(t) \end{bmatrix} = \begin{bmatrix} f_1^1(t) \\ f_2^1(t) \\ f_3^1(t) \end{bmatrix} + \begin{bmatrix} f_1^2(t) \\ f_2^2(t) \\ f_3^2(t) \end{bmatrix} + \begin{bmatrix} f_1^3(t) \\ f_2^3(t) \\ f_3^3(t) \end{bmatrix} \tag{28}$$

where this time domain solution is presented as a function of the Jordan variables. Equation (28) represents the complete solution which includes the linear, second and third order terms in the time domain as a function of Jordan variables initial conditions.

Transforming to the original state variables, the time domain final solution has the form,

$$\begin{bmatrix} y_1(t) \\ y_2(t) \\ y_3(t) \end{bmatrix} = \begin{bmatrix} y_1^0 e^{\lambda_1 t} \\ y_2^0 e^{\lambda_2 t} \\ y_3^0 e^{\lambda_3 t} \end{bmatrix} - \begin{bmatrix} \sum_{k=1}^{N}\sum_{l=1}^{N} h_{2kl}^1 y_k^0 y_l^0 e^{\lambda_1 t} \\ \sum_{k=1}^{N}\sum_{l=1}^{N} h_{2kl}^2 y_k^0 y_l^0 e^{\lambda_2 t} \\ \sum_{k=1}^{N}\sum_{l=1}^{N} h_{2kl}^3 y_k^0 y_l^0 e^{\lambda_3 t} \end{bmatrix} + \begin{bmatrix} \sum_{k=1}^{N}\sum_{l=1}^{N} h_{2kl}^1 y_k^0 y_l^0 e^{(\lambda_k+\lambda_l)t} \\ \sum_{k=1}^{N}\sum_{l=1}^{N} h_{2kl}^2 y_k^0 y_l^0 e^{(\lambda_k+\lambda_l)t} \\ \sum_{k=1}^{N}\sum_{l=1}^{N} h_{2kl}^3 y_k^0 y_l^0 e^{(\lambda_k+\lambda_l)t} \end{bmatrix} \tag{29}$$

$$\begin{bmatrix} x_1(t) \\ x_2(t) \\ x_3(t) \end{bmatrix} = \begin{bmatrix} \Delta E_q^{'}(t) \\ \Delta\delta(t) \\ \Delta\omega(t) \end{bmatrix} = \begin{bmatrix} u_{11} & u_{12} & u_{13} \\ u_{21} & u_{22} & u_{23} \\ u_{31} & u_{32} & u_{33} \end{bmatrix} \begin{bmatrix} y_1(t) \\ y_2(t) \\ y_3(t) \end{bmatrix} \tag{30}$$

Finally, (30) provides the closed-form solutions to the original state variables applying the inverse linear transformation from Jordan variables, just by multiplying by right eigenvectors. Here, the dynamic information given by the modal analysis is maintained at this part of the final solution. Simulation results based on this result are discussed next.

5 Simulation studies

The experiment is conducted assuming a perturbation in the rotor angle. The solution obtained with the modal series technique is compared against the linear approximation, normal forms and the numerical full solution obtained from the nonlinear differential equations that represent the dynamic system. The model of the system consists on stator dynamics represented by the state variable of voltage along the q axis, neglecting d axis effects (one axis flux decay model (20)). The perturbation is initially applied assuming an increment in input torque (mechanical power in the generator); afterwards, a larger increment in the same power joint with another increase in the rotor angle perturbation is reflected as a stress condition. Flow chart of Fig. 4 illustrates the procedure followed to execute the experiment of the case study.

In this case, the perturbation conditions are modified by selecting increases in both rotor angle and mechanical power input in the synchronous generator (stress condition).

The modal analysis is resumed in Table 1. Two oscillatory modes are presented, due to the electromechanical oscillations and a real mode, mainly due to the stator variable $E_q^{'}$. The experiment is performed to compare the solution obtained by modal series against the linear approximation and the direct solution of the nonlinear set of differential equations basically described by (20).

Figure 5 shows the oscillations of the state variables $E_q^{'}$, δ and ω, respectively, when rotor angle and mechanical power input perturbation conditions are applied, i.e., a perturbation in the rotor angle of $\Delta\delta = 10°$ and an increase in the power demand of $P_m = 1.12$ p.u.

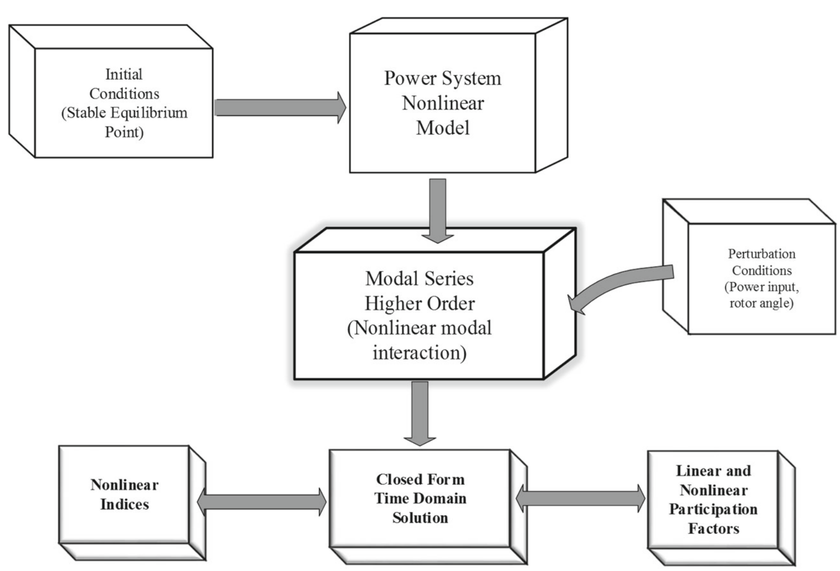

Fig. 4 Flow chart followed to the nonlinear modal series analysis in case studies

Table 1 Modal analysis of SMIB with one flux model

Eigenvalue	Frequency (Hz)	Damping ratio
$\lambda_1 = -0.032834364$	–	–
$\lambda_{2,3} = -0.478749 \pm 5.137238i$	0.817616863444	0.092789977022

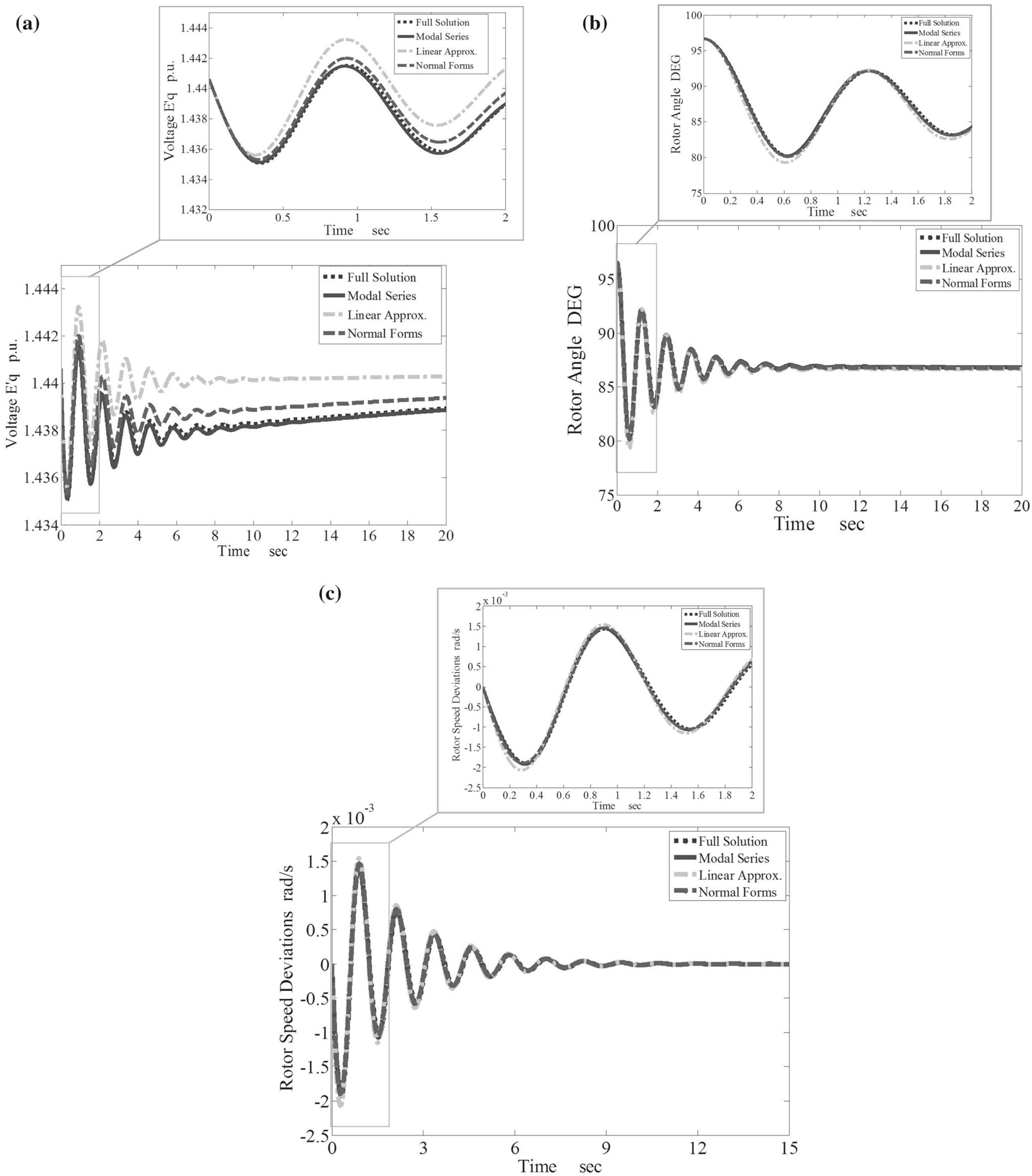

Fig. 5 Rotor angle and speed deviations comparison for a load condition of $P_m = 1.12$ p.u. and $\Delta\delta = 10°$. **a** Voltage E'_q, **b** rotor angle δ, **c** speed rotor ω

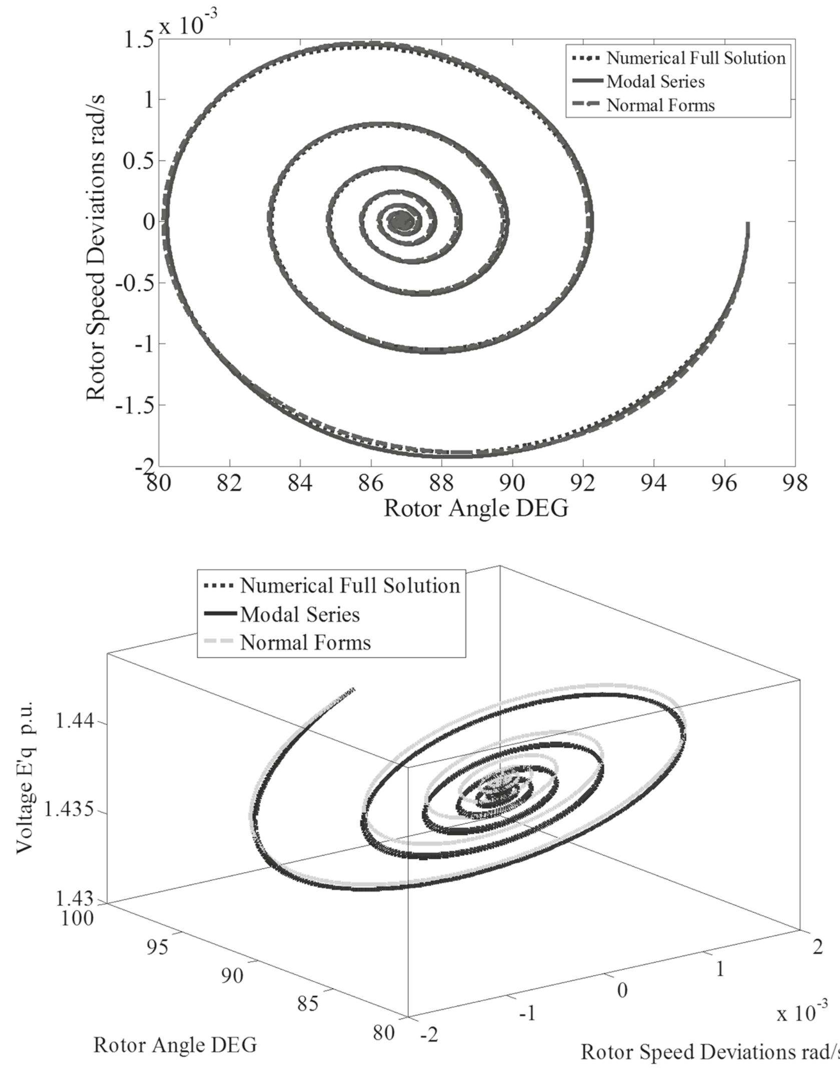

Fig. 6 Rotor angle and speed deviations comparison for a load condition of $P_m = 1.15$ p.u. and $\Delta\delta = 10°$

The perturbation conditions move the system to a stress operation, which is reflected in the oscillations shown in Fig. 5. Please observe that the state variables are oscillating during approximately 5 s, and after that the oscillations tend to die-out reaching a steady state condition. Since the system is stable, even in the presence of the perturbation conditions, it finally reaches this steady state point after a transient period, being larger for the case of voltage $E_q^{'}$. The same Fig. 5 has been conveniently zoomed to show the differences between the solutions with higher detail.

In Fig. 5a, the comparison between the solution obtained with modal series and the full solution with respect to the linear approximation denotes that there is a larger error in the solution calculated by linear approximation, with respect to modal series solution for the state variable of voltage $E_q^{'}$. In this case, the trajectory of modal series solution is very close to the numerical full solution in turn to the linear approximation. In this state variable, the nonlinear contribution is mainly due to the relationship between current and its dependence on rotor angle.

The oscillatory behavior in the generator speed after the change in the initial angle conditions can be observed in Fig. 5b, c. There is a deceleration in the synchronous machine, observed from the decrement in the rotor speed (Fig. 5c) which is accompanied by a decrement in the rotor angle (Fig. 5b) and the magnitude on the voltage $E_q^{'}$ (Fig. 5a). The system keeps oscillating until it reaches the new equilibrium point, which is different in comparison with the initial operating conditions.

The phase plane shown in Fig. 6 demonstrates that the system is stable after the oscillations produced by the disturbance conditions. The rotor angle and rotor speed approach to a stable equilibrium point, which is clearly observable.

Hence, it can be said that the solution obtained with the method of modal series has a good agreement with the

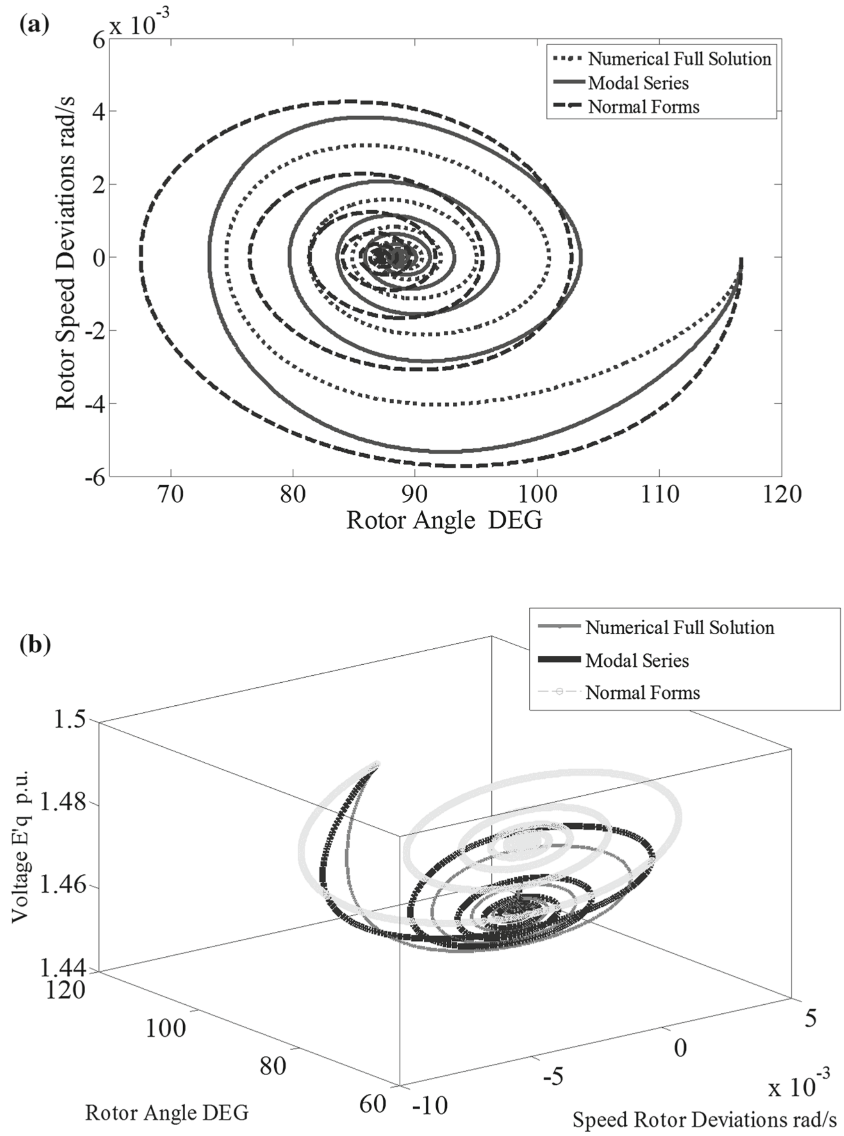

Fig. 7 Phase plane comparison for a load condition of $P_m = 1.5$ p.u. and $\Delta\delta = 30°$. **a** Two dimensional phase plane δ vs ω, **b** three dimensional phase plane δ vs ω vs E'_q

response obtained by the direct numerical solution of the nonlinear power system represented by the set of differential equations (20), in the presence of low perturbation or low stress conditions, since the operation point is near from the initial equilibrium point defined for the linearization of the nonlinear system.

The experiment can be oriented to select different perturbation conditions. The system is now stressed by a step change in the demanded power of the synchronous machine, changing it to $P_m = 1.15$ p.u. together with a perturbation increment of $\Delta\delta = 30°$ is traduced as a high stress operation condition.

In Fig. 7, a three dimensional trajectory followed by the two compared methods, a different solution trajectory is observed, but both solutions finding finally the same final operating point.

Unstable operation increasing stress conditions The next experiment consists on increasing the stress condition by raising the rotor angle above the maximum operating limit ($\Delta\delta = 30°$) described along the case study. Please observe the graphics depicted by Fig. 8, which is showing the rotor angle and speed deviations with operating point based on $\Delta\delta = 31°$ as well as the tridimensional phase plane including the three state variables. It is clear that the system could not operate over the limits which maintains its stability.

This experiment demonstrates that the modal series method approximation could fail when the stress conditions are increased in such a way that the operating point is moved away from the steady state condition. It can be concluded that a stressed power system tends to change the apparent linear behavior, moving the system to oscillate near the edge of unstable conditions.

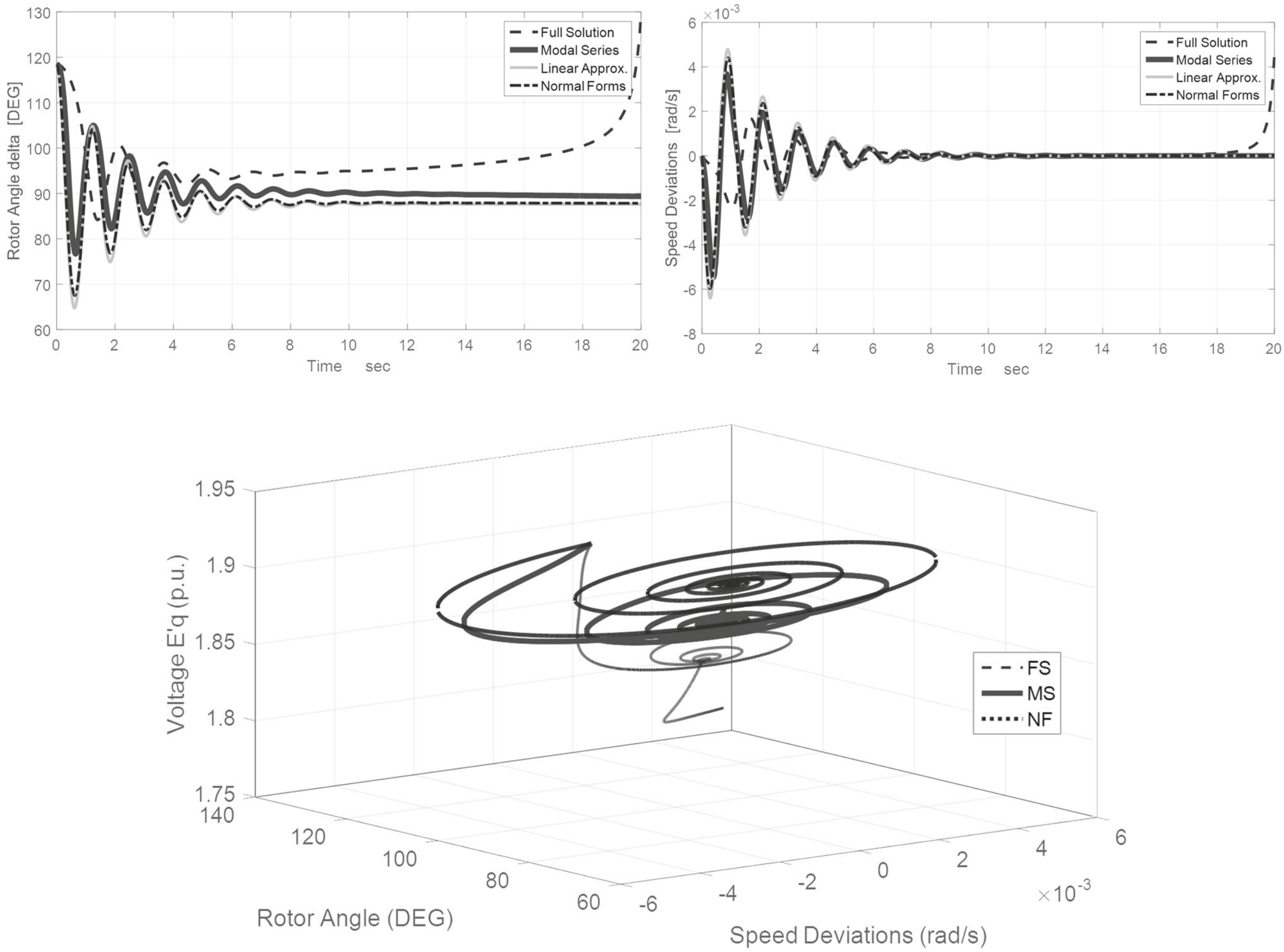

Fig. 8 Comparison for an overstress condition of $P_m = 1.5$ p.u. and $\Delta\delta = 31°$

6 Nonlinear interaction analysis

6.1 Nonlinear indices

The nonlinear contribution of the modal series higher order terms can be measured through nonlinear indices. These indices are basically formed by the coefficients of the modal series.

Index I1 This index determines the second and third nonlinear effects defined by the second and third order coefficients of the modal series. The index indicates a strong modal interaction between modes; it is defined as,

$$\mathrm{I1} = \left| \frac{\max_{k,l} \left| h_{2kl}^{j} y_k(0)\, y_l(0) + h_{3pqr}^{j} y_p^1(0)\, y_q^1(0)\, y_r^1(0) \right|}{y_j(0)} \right| \tag{31}$$

Index I2 A fundamental mode nonlinearity index measures the effect of modal interactions due to the fundamental mode in the original coordinates due to second and third order coefficients.

$$\mathrm{I2}(j) = \frac{\left[y_j(0) - \sum_{k=1}^{n} \sum_{l=1}^{n} h2_{kl}^{j} y_k(0)\, y_l(0) - \sum_{p=1}^{n} \sum_{q=1}^{n} \sum_{r=1}^{n} h_{3pqr}^{j} y_p(0)\, y_q(0)\, y_r(0) \right]}{y_j(0)} \tag{32}$$

Figure 9 shows the levels of both nonlinear indices for the case study of Sect. 5, considering the two scenarios

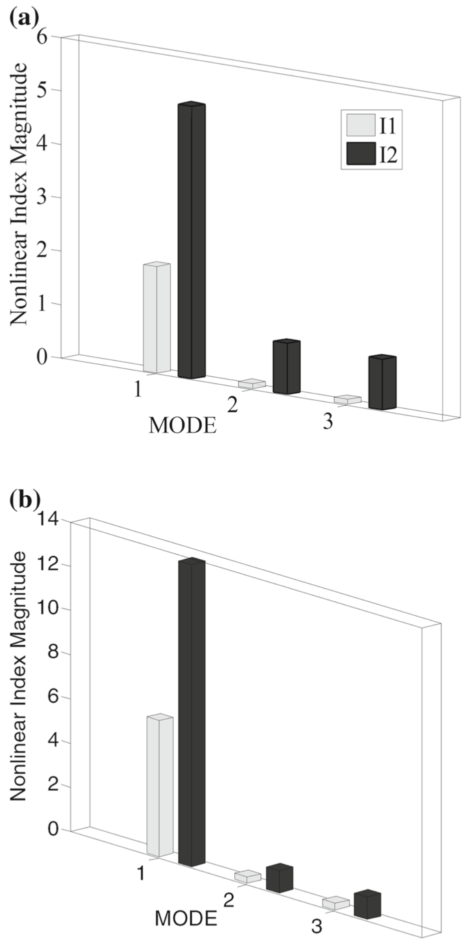

Fig. 9 Nonlinear indices for the case. **a** $P_m = 1.12$ p.u. and $\Delta\delta = 10°$, **b** $P_m = 1.5$ p.u. and $\Delta\delta = 30°$

under study. In both cases, the index with higher level is I2, denoting the biggest magnitude in 5 units (Fig. 9a), while for the second scenario the highest level reaches magnitude in 14 units (Fig. 9b). This result agrees with the behavior observed by Fig. 7 where the system due to the more stressed operating condition, increases its distortion and separation with respect to the linear and full numerical solution.

6.2 Nonlinear participation factors

The participation factors are applied assuming the linear definition and introducing the nonlinear contribution. According to the definition of participation factor, it represents a measure of the participation of the kth machine state trajectory of the ith mode [22].

It is possible to determine the nonlinear participation factors derived from the closed-form solution of the modal series method, that is,

$$\begin{aligned} x_i(t) &= \sum_{j=1}^{n}\left(u_{ij}y_j(0) - \sum_{k=1}^{n}\sum_{l=1}^{n}u_{ij}h_{2kl}^{j}y_k(0)\,y_l(0)\right)e^{\lambda_j t} \\ &+ \sum_{j=1}^{n}\sum_{k=1}^{n}\sum_{l=1}^{n}u_{ij}h_{2kl}^{j}y_k(0)\,y_l(0)\,e^{(\lambda_k+\lambda_l)t} \\ &+ \sum_{p=1}^{n}\sum_{q=1}^{n}\sum_{r=1}^{n}u_{ij}h_{3pqr}^{j}y_p^1(0)\,y_q^1(0)\,y_r^1(0) \\ &\times\left[e^{(\lambda_j)t} - e^{(\lambda_p+\lambda_q+\lambda_r)t}\right] \end{aligned} \tag{33}$$

or, it can be written as,

$$x_i(t) = u1_{ij}e^{\lambda_j t} + u2_{ikl}e^{(\lambda_k+\lambda_l)t} + u3_{pqr}e^{(\lambda_p+\lambda_q+\lambda_r)t} \tag{34}$$

where,

$$\begin{aligned} u1_{ij} &= \left[\sum_{j=1}^{n}u_{ij}y_j(0) - \sum_{k=1}^{n}\sum_{l=1}^{n}u_{2ikl}y_k(0)\,y_l(0)\right] \\ u2_{ikl} &= \sum_{k=1}^{n}\sum_{l=1}^{n}u_{2ikl}y_k(0)\,y_l(0) \\ u3_{pqr} &= \sum_{p=1}^{n}\sum_{q=1}^{n}\sum_{r=1}^{n}u_{ij}h_{3pqr}^{j}y_p(0)\,y_q(0)\,y_r(0) \end{aligned}$$

Equation (34) describes the linear and nonlinear combination of the solution, however, it is necessary to redefine it to obtain the nonlinear participation factors oriented to the closed-form solution obtained through the modal series method. The deduction can be made by considering that the initial condition vector is $x_0 = e_k$, which implies that the Jordan form initial condition can be expressed as,

$$y_{j0} = v_{jk} \tag{35}$$

The participation factors are due to the excitation of one mode at the time, by which it is possible to apply superposition procedure. Thus, the solution for the kth machine state variable (with $x_{i0} = 0$ for all $i \neq k$) is,

$$\begin{aligned} x_i(t) &= \sum_{j=1}^{n}\left[P_{ij} - P2_{kl}^{j}\right]e^{\lambda_j t} + \sum_{j=1}^{n}P2_{kl}^{j}e^{(\lambda_k+\lambda_l)t} \\ &+ \sum_{j=1}^{n}P3_{pqr}^{j}e^{(\lambda_p+\lambda_q+\lambda_r)t} \end{aligned} \tag{36}$$

where,

$$\begin{aligned} P_{ij} &= u_{ij}v_{ji} \\ P2_{kl}^{j} &= \sum_{k=1}^{n}\sum_{l=1}^{n}u_{ij}h2_{kl}^{j}v_{ki}v_{li} \end{aligned}$$

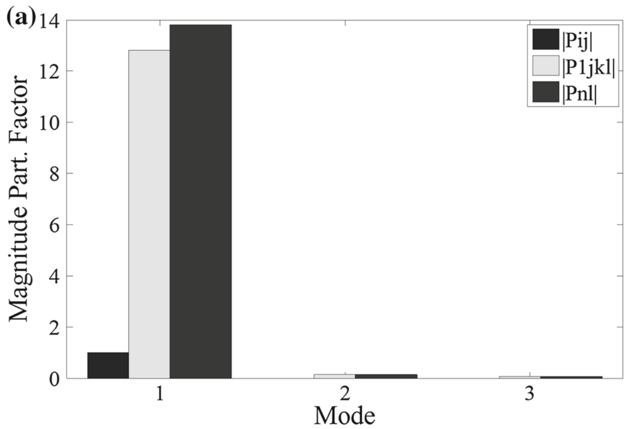

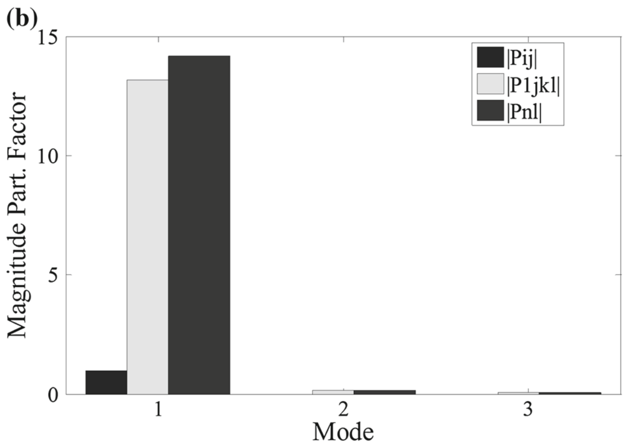

Fig. 10 Nonlinear participation factors. **a** $P_m = 1.12$ p.u. and $\Delta\delta = 10°$, **b** $P_m = 1.5$ p.u. and $\Delta\delta = 30°$

$$P3^j_{pqr} = \sum_{p=1}^{n}\sum_{q=1}^{n}\sum_{r=1}^{n} u_{ij} h3^j_{pqr} v_{pi} v_{qi} v_{ri}$$

$$P1^j_{kl} = P_{ij} - P2^j_{kl}$$

$$P^j nl = P2^j_{kl} + P3^j_{pqr}$$

Figure 10 shows the nonlinear participation factors for the two scenarios of case study, from which the high level of nonlinear contribution $P^j nl$ for the mode 1 can be observed. Even nonlinear participation factor in both scenarios are higher than the linear one, having magnitude near to 14 in the case shown in Fig. 9a, while the case depicted in Fig. 9b shows a level near to 15.

6.3 Cross-frequency

The modal series closed-form solution possess the great advantage to include in an explicit way the cross-frequency content due to each frequency with respect to each mode. Of course, lineal solution cannot represent this situation, since it considers only the contribution of each mode to the time domain response. The importance of these cross-frequencies arises on the contribution of nonlinear action to the behavior of a dynamic system, especially under disturbance conditions or abnormal situations of operation. Also important, apparently, the dynamics of the system is due only to their original parameters, which define the modal analysis. Nevertheless, the excitation of each mode moves the dynamics according to the cross-frequency presented in the modal series. Of course, the weight of each contribution also depends on the value of series coefficients, basically defined, as it was already mentioned in Sect. 6.2, by participation factors.

Table 2 Cross-frequency values for second order terms

k	l	$\lambda_j = \lambda_k + \lambda_l$	Frequency
1	1	-0.06567	0
1	2	$-0.51156003 + 5.133886i$	0.817083376
1	3	$-0.51156003 - 5.133886i$	0.817083376
2	1	$-0.51156003 + 5.133886i$	0.817083376
2	2	$-0.95745135 + 10.2677725i$	1.634166751
2	3	-0.95745	
3	1	$-0.51156003 - 5.133886i$	0.817083376
3	2	-0.95745	
3	3	$-0.95745135 - 10.2677725i$	1.634166751

Tables 2 and 3 describes the total amount of frequencies presented in the modal series, for the case study of Sect. 5. It is easy to identify the frequency content as a sum of modes, being second order (summation of two modes) and third order (summation of three eigenvalues).

7 Discussion

7.1 Computational burden

Computational times are of concern in applications of the power systems solution, mostly when large scale systems are analyzed. In this contribution, only the SMIB test was proved to remark the main steps and differences of the methodology here proposed with respect to other methods, such as NF, being emphasized the inclusion of higher order terms. Some computation times was measured comparing NF, MS and lineal approximation, such as it is described in Table 4. The experiment was performed in a Laptop Core i7, 8 GB RAM, assuming that the case study is simulated 60 s under stable conditions.

It can be observed that the difference between NF and MS is not appreciable since there is less than a half second. However, it is important to highlight that NF method needs a nonlinear transformation and a Newton type algorithm, to find the solution of its new frame reference (basically the normal form new state variables). In contrast, MS is a kind of analytical method indeed, avoiding to determine interme-

Table 3 Cross-frequency values for second order terms

p	q	r	$\lambda_j = \lambda_p + \lambda_q + \lambda_r$	Frequency
1	1	1	-0.098503092	0
1	1	2	$-0.5443944 + 5.1338862i$	0.81708
1	1	3	$-0.5443944 - 5.1338862i$	0.81708
1	2	1	$-0.5443944 + 5.1338862i$	0.81708
1	2	2	$-0.99028571 + 10.267772i$	1.634163
1	2	3	-0.990284	0
1	3	1	$-0.5443944 - 5.1338862i$	0.81708
1	3	2	-0.990285	0
1	3	3	$-0.99028571 - 10.267772i$	1.63417
2	1	1	$-0.5443944 + 5.1338862i$	0.81708
2	1	2	$-0.99028571 + 10.2677725i$	1.634167
2	1	3	-0.990285714	0
2	2	1	$-0.99028571 + 10.2677725i$	1.634167
2	2	2	$-1.43617702 + 15.4016587i$	2.45125
2	2	3	$-1.43617702 + 5.1338862i$	0.817083
2	3	1	-0.990285714	0
2	3	2	$-1.43617702 + 5.1338862i$	0.81708
2	3	3	$-1.43617702 - 5.1338862i$	0.81708
3	1	1	$-0.5443944 - 5.1338862i$	0.81708
3	1	2	-0.990285714	0
3	1	3	$-0.99028571 - 10.2677725i$	1.63417
3	2	1	-0.990285714	0
3	2	2	$-1.43617702 + 5.1338862i$	0.81708
3	2	3	$-1.43617702 - 5.1338862i$	0.81708
3	3	1	$-0.99028571 - 10.2677725i$	1.63417
3	3	2	$-1.43617702 - 5.1338862i$	0.81708
3	3	3	$-1.43617702 - 15.4016587i$	2.45125

Table 4 Computational times comparison between methods

Normal forms	9.091021 s
Modal series	8.549627 s
Linear solution	2.452622 s

diate numerical methods. Of course, due to the absence of nonlinear contributions, linear approximation is the fastest for several seconds.

7.2 Potential applications

The method of MS based on its properties given by multidimensional Laplace transform may be utilized to model transfer functions and input functions effects on the system's nonlinearity. Some other developments could be possible to incorporate, such as sensitivity parameters on nonlinearity characteristics, modal resonance analysis (since it is possible to characterize the system's behavior even when resonance conditions are presented), continuation methods (bifurcations theory), incorporation of renewable energy sources, low inertia conditions, among others.

7.3 Comparative analysis between methods

From the validation observed along the experiment, it can be concluded that the modal series method is always closer to the direct numerical approximation, denoting that the linear approximation can reproduce different trajectories of solution or maintaining near of real solution but with a lower accuracy with respect to the modal series.

The relationship between the rigorous mathematical fundamentals necessary to determine the closed-form solution of a nonlinear power system by the development of the modal series method, may be justified in cases where the system requires the determination of nature of nonlinear modal interaction. The main contribution of modal series lies on the determination of the nonlinear contribution of state variables in modal analysis. The determination of higher order terms in the modal series contributes to increase the accuracy of the solution, and also, increases its capacity to identify the nonlinear contributions above a second order nonlinearity.

Furthermore, a comparison of the modal series method with other methods including the previously proposed modal series [9,10] is detailed in Table 5. The comparison is focused on the modeling detail, analysis capacity and future developments so related with the other approaches.

Future contributions are based on this reasoning, incorporating other elements which contribute with higher nonlinearities, and therefore, modal interaction.

Table 5 Comparison between the modeling capacities of the proposed approach with other formulations

Modeling detail and analysis capability	NF method	Conventional modal series methods	Proposed modal series technique
Higher order transfer function computation	X	Currently limited to second order	Reported
Detailed system modeling/FACTS controllers	Available	Not reported	Reported
Sparsity representation	Available	Not reported	X
Higher order nonlinear solutions	Available (third order)[a]	Second order approximation	Higher order approximation[a]

[a] Theoretically possible up to arbitrary order

8 Conclusions

In this contribution, an analytical methodology based on the modal series technique has been proposed. Based on the modal series previously proposed in [9,10] an extension of the method has been done, which consists on generalizing the method using the theorems of multidimensional Laplace transform and the theorems of association of variables, to analyze the dynamic nonlinear system as an algebraic problem.

The accuracy of the proposed higher order modal series method has been demonstrated through direct comparison against the response obtained with the full set of motion equations, Normal forms method and the linear approximation method.

A detailed description of the higher order modal series terms have been exemplified with a synchronous machine-infinite busbar power system. The nonlinear oscillations produced due to a perturbation on the third order model of the synchronous machine have been analyzed. The main advantages of the method with respect to the linear approximation approach have been detailed.

The theoretical description of the modal series method studied along this contribution, can be applied following the same systematic procedure to the analysis of larger complexity power systems whether higher modeling detail of elements are incorporated or greater number of elements (large scale power systems) are considered.

Appendix A

A.1 Second order terms

Defining the first order expressions in terms of s_1 and s_2 yields,

$$Y_k^1(s_1) = \frac{Y_k^1(0)}{(s_1-\lambda_k)} \quad \text{and} \quad Y_l^2(s_2) = \frac{Y_l^2(0)}{(s_2-\lambda_l)} \tag{A.1}$$

Then,

$$Y_j^2(s_1,s_2) = \sum_{k=1}^{n}\sum_{l=1}^{n} \frac{1}{(s_1+s_2-\lambda_j)} C_{kl}^j \frac{Y_k^1(0)}{(s_1-\lambda_k)} \frac{Y_l^1(0)}{(s_2-\lambda_l)}$$

Applying theorem of association of variables to the function $Y_j^2(s_1,s_2)$ to $Y_j^2(s)$, the second order term becomes

$$Y_j^2(s) = \sum_{k=1}^{n}\sum_{l=1}^{n}\left\{ C_{kl}^j Y_k^1(0)\, Y_l^1(0) \frac{1}{(\lambda_k+\lambda_l-\lambda_j)} \times \left[\frac{1}{(s-\lambda_k-\lambda_l)} - \frac{1}{(s-\lambda_j)}\right]\right\} \tag{A.2}$$

A.2 Third order terms

Recalling,

$$\begin{aligned}(s_1+s_2+s_3)\,Y_j^3(s_1,s_2,s_3) &= \lambda_j Y_j^3(s_1,s_2,s_3) \\ &+ \sum_{k=1}^{n}\sum_{l=1}^{n} C_{kl}^j\left[Y_k^2(s_1,s_2)\,Y_l^1(s_3) + Y_k^1(s_1)\,Y_l^2(s_2,s_3)\right] \\ &+ \sum_{p=1}^{n}\sum_{q=1}^{n}\sum_{r=1}^{n} D_{pqr}^j\left[Y_p^1(s_1)\,Y_q^1(s_2)\,Y_r^1(s_3)\right]\end{aligned}$$

and also, $Y_j^1(s_1) = \frac{Y_j^1(0)}{(s_1-\lambda_j)}$ and

$$Y_j^2(s_1,s_2) = \sum_{k=1}^{n}\sum_{l=1}^{n} \frac{1}{(s_1+s_2-\lambda_j)} C_{kl}^j Y_k^1(s_1)\, Y_l^1(s_2)$$

New indexes are defined to conform third order terms. That is,

$$Y_l^1(s_3) = \frac{Y_l^1(0)}{(s_3-\lambda_l)}; \quad Y_k^1(s_1) = \frac{Y_k^1(0)}{(s_1-\lambda_k)};$$
$$Y_p^1(s_1) = \frac{Y_p^1(0)}{(s_1-\lambda_p)}; \quad Y_q^1(s_2) = \frac{Y_q^1(0)}{(s_2-\lambda_q)};$$
$$Y_r^1(s_3) = \frac{Y_r^1(0)}{(s_3-\lambda_r)}$$

In the same way, second order terms are reindexed as,

$$Y_k^2(s_1,s_2) = \sum_{p=1}^{n}\sum_{q=1}^{n} \frac{1}{(s_1+s_2-\lambda_k)} C_{pq}^k Y_p^1(s_1)\, Y_q^2(s_2) \tag{A.3}$$

$$Y_l^2(s_2,s_3) = \sum_{p=1}^{n}\sum_{q=1}^{n} \frac{1}{(s_2+s_3-\lambda_l)} C_{pq}^l Y_p^1(s_2)\, Y_q^1(s_3) \tag{A.4}$$

Substituting,

$$\begin{aligned}(s_1+s_2+s_3)\,Y_j^3(s_1,s_2,s_3) &= \lambda_j Y_j^3(s_1,s_2,s_3) \\ &+ \sum_{k=1}^{n}\sum_{l=1}^{n} C_{kl}^j\left[\sum_{p=1}^{n}\sum_{q=1}^{n} \frac{1}{(s_1+s_2-\lambda_k)} C_{pq}^k \frac{Y_p^1(0)}{(s_1-\lambda_p)}\right. \\ &\times \frac{Y_q^1(0)}{(s_2-\lambda_q)} \frac{Y_l^1(0)}{(s_3-\lambda_l)} + \frac{Y_k^1(0)}{(s_1-\lambda_k)} \\ &\left.\times \sum_{p=1}^{n}\sum_{q=1}^{n} \frac{1}{(s_2+s_3-\lambda_l)} C_{pq}^l \frac{Y_p^1(0)}{(s_2-\lambda_p)} \frac{Y_q^1(0)}{(s_3-\lambda_q)}\right] \\ &+ \sum_{p=1}^{n}\sum_{q=1}^{n}\sum_{r=1}^{n} D_{pqr}^j\left[\frac{Y_p^1(0)}{(s_1-\lambda_p)} \frac{Y_q^1(0)}{(s_2-\lambda_q)} \frac{Y_r^1(0)}{(s_3-\lambda_r)}\right]\end{aligned} \tag{A.5}$$

Hence, the third order kernel can be redefined as,

$$
\begin{aligned}
Y_j^3(s_1, s_2, s_3) = {} & K_1 N_1(s_1, s_2, s_3) + K_2 N_2(s_1, s_2, s_3) \\
& + K_3 N_3(s_1, s_2, s_3)
\end{aligned}
$$

with

$$
\begin{aligned}
& N_1(s_1, s_2, s_3) \\
& = \frac{1}{(s_1+s_2+s_3-\lambda_j)(s_1+s_2-\lambda_k)(s_1-\lambda_p)(s_2-\lambda_q)(s_3-\lambda_l)} \\
& N_2(s_1, s_2, s_3) \\
& = \frac{1}{(s_1+s_2+s_3-\lambda_j)(s_2+s_3-\lambda_l)(s_1-\lambda_k)(s_2-\lambda_p)(s_3-\lambda_q)} \\
& N_3(s_1, s_2, s_3) \\
& = \frac{1}{(s_1+s_2+s_3-\lambda_j)(s_1-\lambda_p)(s_2-\lambda_q)(s_3-\lambda_r)}
\end{aligned}
$$

A.3 Association of variables

To solve the kernels $N_1(s_1, s_2, s_3)$ and $N_2(s_1, s_2, s_3)$, it is possible to use the corollary proposed by [17]. The corollary fits to $(i-1)$st reduction and expansion of a n-dimensional kernels of the form,

$$
\begin{aligned}
& Z_n(s_1, s_2, \ldots, s_n) \\
& = \frac{G_n(s_1, s_2, \ldots, s_n)}{\prod_{k1=1}^{K11}(s_1+s_2+\cdots+s_i+x_{k1})} \\
& \cdot \frac{1}{\prod_{k2=K11+1}^{K22}\left(s_1+s_2+\cdots+s_i+\sum\limits_{m>i} s_m + x_{k2}\right)} \\
& \cdot \frac{1}{\prod_{j1=1}^{J11}(s_1+\alpha_{j1})\prod_{j2=1}^{J22}(s_2+\beta_{j2})\cdots\prod_{ji=1}^{Jii}(s_i+\eta_{ji})}
\end{aligned}
\tag{A.6}
$$

where $G_n(s_1, s_2, \ldots, s_n)$ is the ratio of a polynomial in n variables to a polynomial in the $n-i$ variables $i+1, i+2, \ldots, n-1$ and n. The corollary is described by [18].

Hence, applying the corollary to kernels $N_1(s_1, s_2, s_3)$ and $N_2(s_1, s_2, s_3)$, manipulating some algebraic expressions and defining them in terms of a single Laplace domain by association of variables theorems as,

$$
\begin{aligned}
N_1(s) = {} & \frac{1}{(\lambda_j-\lambda_p-\lambda_q-\lambda_l)}\left[\frac{1}{(\lambda_j-\lambda_l-\lambda_k)}\frac{1}{(s-\lambda_j)}\right. \\
& \left. -\frac{1}{(\lambda_p+\lambda_q-\lambda_k)}\frac{1}{(s-\lambda_p-\lambda_q-\lambda_l)}\right]
\end{aligned}
\tag{A.7}
$$

In the same way are obtained the rest of kernels $N_2(s)$ and $N_3(s)$. Finally, the kernel $N_1(s_1, s_2, s_3)$ is reduced following the approach proposed in [18]. Thus, the final solution of third order terms expressed as a single Laplace transform variable is,

$$
\begin{aligned}
& Y_j^3(s) = K_1 N_1(s) + K_2 N_2(s) + K_3 N_3(s) \\
& Y_j^3(s) = \frac{1}{(\lambda_j-\lambda_p-\lambda_q-\lambda_l)} \\
& \quad \times \left\{ \begin{array}{l} K_1\left[\frac{1}{(\lambda_j-\lambda_l-\lambda_k)}\frac{1}{(s-\lambda_j)} - \frac{1}{(\lambda_p+\lambda_q-\lambda_k)}\frac{1}{(s-\lambda_p-\lambda_q-\lambda_l)}\right] \\ +K_2\frac{1}{(\lambda_p+\lambda_q-\lambda_l)}\left[\frac{1}{(s-\lambda_j)} - \frac{1}{(s_1-\lambda_p-\lambda_q-\lambda_k)}\right] \end{array} \right\} \\
& \quad + K_3\frac{1}{(\lambda_j-\lambda_p-\lambda_q-\lambda_r)} \\
& \quad \times \left[\frac{1}{(s-\lambda_j)} - \frac{1}{(s-\lambda_p-\lambda_q-\lambda_r)}\right]
\end{aligned}
\tag{A.8}
$$

Appendix B

B.1 First order terms

The first order or linear terms are defined as,

$$
f_1(\mathbf{x}) = \mathbf{A}\mathbf{x}, \quad \text{with, } \mathbf{A} = \begin{bmatrix} \frac{\partial f_1}{\partial E_q'} & \frac{\partial f_1}{\partial \delta} & \frac{\partial f_1}{\partial \omega} \\ \frac{\partial f_2}{\partial E_q'} & \frac{\partial f_2}{\partial \delta} & \frac{\partial f_2}{\partial \omega} \\ \frac{\partial f_3}{\partial E_q'} & \frac{\partial f_1}{\partial \delta} & \frac{\partial f_1}{\partial \omega} \end{bmatrix}_{X=X_{\mathrm{SEP}}}
\tag{B.1}
$$

$$
\mathbf{A} = \left[\begin{array}{l|l|l} \frac{1}{T_{d0}'}[K_1-1] & \frac{1}{T_{d0}'}[K_1 V_b \sin\delta] & 0 \\ \hline 0 & 0 & 1 \\ \hline \frac{\omega_0}{2H}\begin{bmatrix} K_2 V_b \sin\delta + \\ K_3 V_b \sin\delta \end{bmatrix} & \frac{\omega_0}{2H}\begin{bmatrix} K_2 E_q' V_b \cos\delta + \\ K_3 V_b^2 \sin^2\delta + \\ K_3\left(E_q' - V_b\cos\delta\right) V_b \cos\delta \end{bmatrix} & -\frac{\omega_0}{2H} D \end{array}\right]_{X=X_{\mathrm{SEP}}}
\tag{B.2}
$$

where,

$$
\begin{aligned}
& K_1 = -\frac{x_d - x_d'}{x_d' + x_{ep}}, \quad K_2 = -\frac{1}{x_q + x_{ep}} \\
& K_3 = -\frac{x_q - x_d'}{(x_d' + x_{ep})(x_q + x_{ep})}, \quad x_{ep} = x_t + x_l
\end{aligned}
$$

Applied to the case of the third order power system under study, the state matrix has the form described by (B.2).

B.2 Second order terms

The second order terms result from the matrix product,

$$
f_2(\mathbf{x}) = \frac{1}{2}\begin{bmatrix} \mathbf{x}^{\mathrm{T}}\mathbf{H}^1\mathbf{x} \\ \mathbf{x}^{\mathrm{T}}\mathbf{H}^2\mathbf{x} \\ \mathbf{x}^{\mathrm{T}}\mathbf{H}^3\mathbf{x} \end{bmatrix} = \frac{1}{2}\begin{bmatrix} \sum\limits_{k=1}^{n}\sum\limits_{l=1}^{n} H_{kl}^1 x_k x_l \\ \sum\limits_{k=1}^{n}\sum\limits_{l=1}^{n} H_{kl}^2 x_k x_l \\ \sum\limits_{k=1}^{n}\sum\limits_{l=1}^{n} H_{kl}^3 x_k x_l \end{bmatrix}
\tag{B.3}
$$

With, $H^{j}=\begin{bmatrix} \frac{\partial^2 f_j}{\partial E_q' \partial E_q'} & \frac{\partial^2 f_j}{\partial E_q' \partial \delta} & \frac{\partial^2 f_j}{\partial E_q' \partial \omega} \\ \frac{\partial^2 f_j}{\partial \delta_q \partial E_q'} & \frac{\partial^2 f_j}{\partial \delta \partial \delta_q} & \frac{\partial^2 f_j}{\partial \delta \partial \omega} \\ \frac{\partial^2 f_j}{\partial \omega \partial E_q'} & \frac{\partial^2 f_j}{\partial \omega \partial \delta} & \frac{\partial^2 f_j}{\partial \omega \partial \omega} \end{bmatrix}_{X=X_{\mathrm{SEP}}}$

which has the form,

$$H=\left[\begin{array}{ccc|ccc|ccc} 0 & 0 & 0 & 0 & 0 & 0 & 0 & H_{(1,8)} & 0 \\ 0 & H_{(2,2)} & 0 & 0 & 0 & 0 & H_{(2,7)} & H_{(2,8)} & 0 \\ 0 & 0 & 0 & 0 & 0 & 0 & 0 & 0 & 0 \end{array}\right]$$

$$H_{(1,8)}=\frac{\omega_r}{2H}\left(-K_2 V_b \cos\delta+K_3 V_b \cos\delta\right)$$

$$H_{(2,2)}=-\frac{1}{T_{d0}'} K_1 V_b \cos\delta;$$

$$H_{(2,7)}=\frac{\omega_r}{2H}\left(K_2 V_b \cos\delta+K_3 V_b \cos\delta\right)$$

$$H_{(2,8)}=\frac{\omega_r}{2H}\left\{\begin{array}{l} -K_2 E_q' V_b \sin\delta \\ \quad +3K_3 V_b^2 \sin\delta\cos\delta \\ \quad +K_4(E_q'-V_b\cos\delta) V_b \sin\delta \end{array}\right\}$$

$$K_4=\frac{x_q-x_d'}{(x_d'-x_{ep})(x_q+x_{ep})}$$

B.3 Third order terms

In the same way as the second order terms, the third order derivative of Taylor series expansion results in the matrix equation,

$$f_3(\mathbf{x})=\frac{1}{6}\begin{bmatrix} \mathbf{x}^{\mathrm{T}}\mathbf{H}_3^1 \begin{bmatrix} \mathbf{x} & \mathbf{0} & \mathbf{0} \\ \mathbf{0} & \mathbf{x} & \mathbf{0} \\ \mathbf{0} & \mathbf{0} & \mathbf{x} \end{bmatrix}\mathbf{x} \\ \mathbf{x}^{\mathrm{T}}\mathbf{H}_3^2 \begin{bmatrix} \mathbf{x} & \mathbf{0} & \mathbf{0} \\ \mathbf{0} & \mathbf{x} & \mathbf{0} \\ \mathbf{0} & \mathbf{0} & \mathbf{x} \end{bmatrix}\mathbf{x} \\ \mathbf{x}^{\mathrm{T}}\mathbf{H}_3^3 \begin{bmatrix} \mathbf{x} & \mathbf{0} & \mathbf{0} \\ \mathbf{0} & \mathbf{x} & \mathbf{0} \\ \mathbf{0} & \mathbf{0} & \mathbf{x} \end{bmatrix}\mathbf{x} \end{bmatrix}$$

$$=\frac{1}{6}\begin{bmatrix} \sum_{k=1}^{n}\sum_{l=1}^{n}\sum_{m=1}^{n} H_{3klm}^1 x_k x_l x_m \\ \sum_{k=1}^{n}\sum_{l=1}^{n}\sum_{m=1}^{n} H_{3klm}^2 x_k x_l x_m \\ \sum_{k=1}^{n}\sum_{l=1}^{n}\sum_{m=1}^{n} H_{3klm}^3 x_k x_l x_m \end{bmatrix} \tag{B.4}$$

where the third order matrix is defined by

$$\mathbf{H}_3^j=\begin{bmatrix} \frac{\partial^3 f_j}{\partial E_q'^3} & \frac{\partial^3 f_j}{\partial E_q'^2 \partial\delta} & \frac{\partial^3 f_j}{\partial E_q'^2 \partial\omega} & \frac{\partial^3 f_j}{\partial E_q' \partial\delta \partial E_q'} & \frac{\partial^3 f_j}{\partial E_q' \partial\delta^2} & \frac{\partial^3 f_j}{\partial E_q' \partial\delta \partial\omega} & \frac{\partial^3 f_j}{\partial E_q' \partial\omega \partial E_q'} & \frac{\partial^3 f_j}{\partial E_q' \partial\omega \partial\delta} & \frac{\partial^3 f_j}{\partial E_q' \partial\omega^2} \\ \frac{\partial^3 f_j}{\partial\delta \partial E_q'^2} & \frac{\partial^3 f_j}{\partial\delta \partial E_q' \partial\delta} & \frac{\partial^3 f_j}{\partial\delta \partial E_q' \partial\omega} & \frac{\partial^3 f_j}{\partial\delta^2 \partial E_q'} & \frac{\partial^3 f_j}{\partial\delta^3} & \frac{\partial^3 f_j}{\partial\delta^2 \partial\omega} & \frac{\partial^3 f_j}{\partial\delta \partial\omega \partial E_q'} & \frac{\partial^3 f_j}{\partial\delta \partial\omega \partial\delta} & \frac{\partial^3 f_j}{\partial\delta \partial\omega^2} \\ \frac{\partial^3 f_j}{\partial\omega \partial E_q'^2} & \frac{\partial^3 f_j}{\partial\omega \partial E_q' \partial\delta} & \frac{\partial^3 f_j}{\partial\omega \partial E_q' \partial\omega} & \frac{\partial^3 f_j}{\partial\omega \partial\delta \partial E_q'} & \frac{\partial^3 f_j}{\partial\omega \partial\delta^2} & \frac{\partial^3 f_j}{\partial\omega \partial\delta \partial\omega} & \frac{\partial^3 f_j}{\partial\omega^2 \partial E_q'} & \frac{\partial^3 f_j}{\partial\omega^2 \partial\delta} & \frac{\partial^3 f_j}{\partial\omega^3} \end{bmatrix}_{X=X_{\mathrm{SEP}}} \tag{B.5}$$

Fitting to this case study, $\mathbf{H}_3^j$ matrices have the form,

$$\begin{aligned} \mathbf{H}_3^1 &= \left[\begin{array}{ccc|ccc|ccc} 0 & 0 & 0 & 0 & 0 & 0 & 0 & 0 & 0 \\ 0 & 0 & 0 & 0 & H_{(2,5)}^1 & 0 & 0 & 0 & 0 \\ 0 & 0 & 0 & 0 & 0 & 0 & 0 & 0 & 0 \end{array}\right]_{X=X_{\mathrm{SEP}}} \\ \mathbf{H}_3^2 &= \mathrm{zeros}\,(3\times 9) \\ \mathbf{H}_3^3 &= \left[\begin{array}{ccc|ccc|ccc} 0 & 0 & 0 & 0 & H_{(1,5)}^3 & 0 & 0 & 0 & 0 \\ 0 & H_{(2,2)}^3 & 0 & H_{(2,4)}^3 & H_{(2,5)}^3 & 0 & 0 & 0 & 0 \\ 0 & 0 & 0 & 0 & 0 & 0 & 0 & 0 & 0 \end{array}\right]_{X=X_{\mathrm{SEP}}} \end{aligned} \tag{B.6}$$

Appendix C

Test system data:

$$H=3.5\,MW/MVA,\quad D=10\text{ p.u.},\quad x_d'=0.3\text{ p.u.}$$
$$x_t=0.15\text{ p.u.},\quad x_l=0.8\text{ p.u.}$$

References

1. Thapar J, Vittal V, Kliemann W, Fouad AA (1997) Application of the normal form of vector fields to predict interarea separation in power systems. IEEE Trans Power Syst 12(2):844–850
2. Jang G, Vittal V, Kliemann W (1998) Effect of nonlinear modal interaction on control performance: use of normal forms technique in control design part I: general theory and procedure. IEEE Trans Power Syst 13(2):401–407
3. Vittal V, Bhatia N, Fouad AA (1991) Analysis of the inter-area mode phenomenon in power systems following large disturbances. IEEE Trans Power Syst 6(4):1515–1521
4. Sanchez-Gasca JJ, Vittal V, Gibbard MJ, Messina AR, Vowles DJ, Liu S, Annakage UD (2005) Inclusion of higher-order terms for small-signal (modal) analysis: committee report—task force on assessing the need to include higher order terms for small-signal (modal) analysis. IEEE Trans Power Syst 20(4):1886–1904
5. Barocio E, Messina AR (2003) Normal form analysis of stressed power systems: incorporation of SVC models. Electr Power Energy Syst 25:79–90
6. Betancourt RJ, Barocio E, Arroyo J, Messina AR (2006) A real normal form approach to the study of resonant power systems. IEEE Trans Power Syst 21(1):431–432
7. Amano H, Kumano T, Inoue T (2006) Nonlinear stability indexes of power swing oscillation using normal form analysis. IEEE Trans Power Syst 21(2):825–834
8. Lomei H, Sutanto D, Muttaqi KM, Assili M (2015) A new approach to reduce the non-linear characteristics of a stressed power system by using the normal form technique in the control design of the

excitation system. In: Industry applications society annual meeting, 2015 IEEE, Addison, TX, pp 1–6
9. Shanechi HM, Pariz N, Vaahedi E (2003) General nonlinear modal representation of large scale power systems. IEEE Trans Power Syst 18(3):1103–1109
10. Pariz N, Shanechi HM, Vaahedi E (2003) Explaining and validating stressed power systems behavior using modal series. IEEE Trans Power Syst 18(2):778–785
11. Wu FX, Wu H, Han ZX, Gan DQ (2007) Validation of power system nonlinear modal methods. Electr Power Syst Res 77(10):1418–1424
12. Chen W, Bi T, Yang Q, Deng J (2010) Analysis of nonlinear torsional dynamics using second-order solutions. IEEE Trans Power Syst 25(1):423–432
13. Rodriguez O, Medina A, Roman-Messina A, Fuerte-Esquivel CR (2009) The modal series method and multi-dimensional Laplace transforms for the analysis of nonlinear effects in power systems dynamics. In: IEEE GM2009. Calgary, Alberta, Canada
14. Rodríguez O, Medina A, Andersson G (2015) Closed-form analytical characterisation of non-linear oscillations in power systems incorporating unified power flow controller. IET Gener Transm Distrib 9(11):1019–1032
15. Debnath J, Chandra Debnath N (1989) Theorems on association of variables in multidimensional Laplace transforms. Int J Math Math Sci 12(2):363–376
16. Rugh WJ (1981) Nonlinear system theory, the Volterra/Wiener approach. The John Hopkins University Press, Baltimore
17. Crum LA, Heinen JA (1974) Simultaneous reduction and expansion of multidimensional Laplace transform kernels. SIAM J Appl Math 26(4):753–771
18. Lubbock JK, Bansal VS (1969) Multidimensional Laplace transforms for solution of nonlinear equations. Proc Inst Electr Eng 116(12):2075–2082
19. Rodriguez O, Medina A (2011) Nonlinear transfer function based on forced response modal series analysis. In: North American power symposium NAPS 2011, pp 1–8, 4–6 Aug 2011
20. Martínez I, Messina AR, Barocio E (2004) Perturbation analysis of power systems: effects of second and third-order nonlinear terms on system dynamic behavior. Electr Power Syst Res 71(2):159–167
21. Sauer P, Pai MA (1998) Power system dynamics and stability. Prentice Hall, Upper Saddle River
22. Perez-Arriaga IJ, Verghese GC, Schweppe FC (1982) Selective modal analysis with applications to electric power systems, Part I and II. IEEE Trans Power Appar Syst PAS-101(9):3117–3134